Age (Dordr). 2015 Feb; 37(1): 12.
Published online 2015 Feb 8. doi: 10.1007/s11357-015-9747-3
PMCID: PMC4320125
PMID: 25663420

Amyloid and tau pathology of familial Alzheimer's disease APP/PS1 mouse model in a senescence phenotype background (SAMP8)

D. Porquet,[#] P. Andrés-Benito,[#] C. Griñán-Ferré, A. Camins, I. Ferrer, A. M. Canudas, J. Del Valle, and Mercè Pallàs[✉]

Secció de Farmacologia, Departament Farmacologia i Química Terapèutica, Facultat de Farmàcia, Institut de Biomedicina (IBUB), Universitat de Barcelona (UB), Av. Diagonal 643, 08028 Barcelona, Spain
Grup de Neuroplasticitat i Regeneració, Institut de Neurociències i Departament de Biologia cellular, Fisiologia i Immunologia, Universitat Autònoma de Barcelona (UAB), 08193 Bellaterra, Barcelona Spain
Institut de Neuropatologia de l'Hospital Universitari de Bellvitge (HUB), Institut d'Investigació Biomèdica de Bellvitge (IDIBELL), Universitat de Barcelona (UB), 08907 Bellvitge, Barcelona Spain
Centros de Investigación Biomédica en Red de Enfermedades Neurodegenerativas (CIBERNED), Madrid, Spain
Mercè Pallàs, Phone: (+34) 934024531, Email: pallas@ub.edu.
[✉]Corresponding author.
[#]Contributed equally.

Received 2014 Nov 10; Accepted 2015 Jan 22.

Abstract

Go to:

The amyloid precursor protein/presenilin 1 (APP/PS1) mouse model of Alzheimer's disease (AD) has provided robust neuropathological hallmarks of familial AD-like pattern at early ages, whereas senescence-accelerated mouse prone 8 (SAMP8) has a remarkable early senescence phenotype with pathological similarities to AD. The aim of this study was the investigation and characterization of cognitive and neuropathological AD markers in a novel mouse model that combines the characteristics of the APP/PS1 transgenic mouse model with a senescence-accelerated background of SAMP8 mice. Initially, significant differences were found regarding amyloid plaque formation and cognitive abnormalities. Bearing these facts in mind, we determined a general characterization of the main AD brain molecular markers, such as alterations in amyloid pathway, neuroinflammation, and hyperphosphorylation of tau in these mice along their lifetimes. Results from this analysis revealed that APP/PS1 in SAMP8 background mice showed alterations in the pathways studied in comparison with SAMP8 and APP/PS1, demonstrating that a senescence-accelerated background exacerbated the amyloid pathology and maintained the cognitive dysfunction present in APP/PS1 mice. Changes in tau pathology, including the activity of cyclin-dependent kinase 5 (CDK5) and glycogen synthase kinase 3 β (GSK3β), differs, but not in a parallel manner, with amyloid disturbances.

Keywords: Familial Alzheimer's disease (fAD), Aging, β-Amyloid, Tau hyperphosphorylation, Cognitive impairment

Introduction

Go to:

Aging-associated processes, neurodegenerative diseases the most prevalent of these, result mainly from the deleterious effects of time on cellular mechanisms (Smith et al. 1996; Agarwal et al. 2003). The main neurodegenerative diseases are Alzheimer's (AD), Parkinson's (PD), Huntington's (HD), and amyotrophic lateral sclerosis (ALS) (Zhu et al. 2004, 2007), with AD being the most prevalent and one of the most studied of these and characterized by mild cognitive impairment, deficits in short-term

memory, spatial memory loss, and subtle emotional imbalances (Enserink 1998), and ultimately causing death (Pimplikar 2009).

With regard to histopathology, changes in AD brains include neuronal and synaptic loss and the appearance of two basic hallmarks: senile plaque (SP) formation by accumulation of extracellular of β-amyloid protein (Aβ) (Glenner and Wong 1984; Braak and Braak 1991, 1998), and intracellular neurofibrillary tangles (NFT) formation by accumulation of hyperphosphorylated tau protein (Bancher et al. 1989; Braak and Braak 1995).

Over time, AD could be divided into two clinical phases, depending on the age of onset (Koedam et al. 2010). On the one hand, it is possible to find a familial Alzheimer's disease (fAD), which was usually defined for individuals <65 years of age, accounting for 5 % of all cases (Harvey 2003) and directly linked with highly penetrant autosomal dominant mutations in one of three different genes: the presenilin 1 (*PS1*) gene, the presenilin 2 (*PS2*) gene, or the amyloid precursor protein (*APP*) gene (Campion et al. 1999). On the other hand, it is possible to find sporadic Alzheimer's disease (sAD), which accounts for approximately 95 % of all AD cases and which likely results from the complex interplay of molecular, environmental, and genetic factors (Guimerà et al. 2002; Koedam et al. 2010; Feng and Wang 2012).

Due to the high degree of variability and its scattered etiology, many problems have had to be overcome in the last two decades of research on aging and associated neurodegenerative diseases. The models usually used are mice that are genetically modified by human gene insertions with the main proteins associated with AD (APP, PS1, PS2, and tau) or tau kinase overexpression (cyclin-dependent kinase 5 [CDK5] or glycogen synthase kinase 3 β [GSK3β]) (Lucas et al. 2001; Piedrahita et al. 2010). However, none of the numerous animal models reliably reflect what occurs in humans because AD should be considered a polyetiologic disease (Itzhaki 1994) that is caused by disruption of a wide range of molecular mechanisms. At the same time, it should be borne in mind that the mutations introduced into transgenic models are related with mutations linked with fAD cases; thus, animal models will not be representative of the vast majority of cases of the sporadic type of Alzheimer's disease (Guimerà et al. 2002; Koedam et al. 2010; Feng and Wang 2012).

It is noteworthy that advanced age is the most important risk factor for the development of sAD (Wisniewski et al. 1996). It was thought that acquiring a more representative model of the sAD type will thus lead to a better understanding of the relationship among changes in homeostasis in senescence and AD, and at this stage, Lok et al. (2013a, b) presented a combined model of AD (amyloid precursor protein/presenilin 1 (APP/PS1)) with senescence-accelerated mouse prone 8 (SAMP8), a representative model of aging, to obtain a new model that displays the characteristics of both.

On the other hand, we decided to use the double transgenic APP/PS1 mice as an animal model of AD, which can contribute cerebral pathologic changes similar to those in humans and which can be used to simulate neuropathologic changes such as SP formation, neuroglial cell proliferation, and decrease of synapses and dendrites (Irizarry et al. 1997; Games et al. 2006; Codita et al. 2006). APP/PS1 mice express a chimeric mouse/human APP bearing the Swedish mutation (Mo/HuAPP695swe) (Borchelt et al. 1996; Dewachter et al. 2000), exhibiting a marked elevation in Aβ protein level and Aβ deposition in the cerebral cortex and hippocampus and developing similar neuropathological hallmarks to those observed in AD brains (Games et al. 1995), and a mutant human PS1-ΔE9 (Borchelt et al. 1996; Campion et al. 1999) that displays an increased Aβ42 peptide formation, potentiating amyloid deposition through superactivation of the PS1 catalytic form (McGowan et al. 1999).

SAMP8 is characterized by deficits in learning and memory (Takeda et al. 1981; Miyamoto et al. 1986; Takeda 2009), emotional disorders such as reduced anxiety-like behavior (Miyamoto et al. 1992; Markowska et al. 1998), impaired immune response, etc. (Yagi et al. 1988; Flood and Morley 1998) at an earlier age. More importantly, this strain is increasingly being recognized as a model of age-related AD (Pallas et al. 2008; Morley et al. 2012) because it shows an AD-related pathology with aging such as alterations in APP processing by secretases (Morley et al. 2000, 2002), increases in Aβ (Del Valle et al. 2010) and in other protein aggregates (Manich et al. 2011), cerebral amyloid angiopathy (del Valle et

al. 2011), and increases in tau hyperphosphorylation (Canudas et al. 2005).

Thus, the goal of the present work is to examine key biochemical and functional characteristics of this disease, including the study of memory impairment, and amyloid and tau pathologies, combining the features of the accelerated senescence background of SAMP8 mice and the APPswe/PS1-ΔE9 mutations of APP/PS1 mice, and this mouse was APP/PS1/SAMP8 and denominated as SHAP.

Materials and methods

Go to:

Animals

SAMP8 and APP/PS1 mouse strains were commercially available (Harlan Laboratories). The generation of APP/PS1 mice expressing human mutated forms of APP and PS1-ΔE9 has already been described (Borchelt et al. 1996). New model strains, SHAP(+) and SHAP(−), were obtained through crossing the male APP/PS1 ($n = 5$) and the female SAMP8 ($n = 13$). All mice have been backcrossed to their parental strain for at least five generations, and once the progeny was obtained ($n = 92$), the animals were genotyped by conventional polymerase chain reaction (PCR), following the protocol proposed by Jackson Laboratory for APP/PS1, resulting in 57.6 % SHAP(+) ($n = 53$), with both transgenes, and 42.4 % SHAP(−) ($n = 39$), without any transgene.

Experimental procedures were carried out with the following four mice strain groups at 3, 6, 9, and 12 months (12 experimental groups): SAMP8 ($n = 12$, three for each age), APP/PS1 ($n = 16$, four for each age), SHAP(+) ($n = 16$, four for each age), and SHAP(−) ($n = 12$, three for each age).

All of the animals were fed a standard chow (2018 Teklad Global 18 % Protein Rodent Maintenance Diet, Harlan) and water ad libitum and were maintained under standard temperature conditions (22 ± 2 °C) of 12-h light/12-h dark cycles (300 lx/0 lx) and at a relative humidity of 55 %. Studies were performed in accordance with the institutional guidelines for the care and use of laboratory animals (European Communities Council Directive 86/609/EEC) established by the Ethical Committee for Animal Experimentation at the University of Barcelona.

Object recognition test

Nine- and 12-month-old SAMP8, APP/PS1, SHAP(+), and SHAP(−) animals were placed in a 90°, two-arm, 25-cm-long, 20-cm-high, and 5-cm-wide black maze. Light intensity in the middle of the field was 30 lx. The objects to be discriminated were made of plastic (object A, 5.25 cm in height, and object B, 4.75 cm in height). For the first 3 days, the mice were individually acclimatized to the apparatus for 10 min. On day 4, the animals were submitted to a 10-min acquisition trial (first trial), during which they were placed in the maze in the presence of two identical novel objects (A + A or B + B), which were localized at the end of each arm. A 10-min retention trial (second trial) occurred 2 h later. During this second trial, objects A and B were placed in the maze, and the time that the animal explored the new object (t_n) and the old object (t_o) was recorded, and an object discrimination index (DI) was calculated by comparing the exploration time of the familiar and the novel objects during the test, defined as $(t_n - t_o)/(t_n + t_o)$. Understanding as exploration of an object was directing the nose at a distance ≥2 cm to the object and/or touching it with the nose, while turning around or sitting on the object was not considered as an exploration (Antunes and Biala 2012). In this case, as well as in most studies, exploration was defined as the orientation of the animal's snout toward the object, sniffing or touching with the snout, while running around the object and sitting or climbing on it was not recorded as exploration (Bahrick et al. 1997; Aubele et al. 2008). In order to avoid object preference biases, objects A and B were counterbalanced so that one half of the animals in each experimental group were first exposed to object A and then to object B, whereas the other one half saw first object B and then object A. The maze and the objects were cleaned with 96° ethanol between experiments to eliminate olfactory cues.

Brain processing

Animals were anesthetized with 80 mg/kg of sodium pentobarbital and intracardially perfused with saline serum. Afterward, brains were dissected and separated sagitally in two hemispheres: one for immunohistochemistry and the other for protein extraction. Immunohistochemistry brains were frozen by immersion in isopentane, chilled on dry ice, and stored at −80 °C until sectioning. Thereafter, frozen brains were embedded in OCT cryostat-embedding compound (Tissue-Tek, Torrance, CA, USA), cut into 20-µm-thick sections on a cryostat (Leica Microsystems, Germany) at −18 °C, and placed on slides. Slides containing brain sections were fixed with acetone for 10 min at 4 °C, allowed to dry at room temperature, and then frozen at −20 °C until further staining. The remaining hemispheres were dissected in total cortex and total hippocampus and stored at −80 °C until protein extraction and Aβ quantification.

Thioflavin S staining

Slides were allowed to defreeze at room temperature and then were rehydrated with phosphate-buffered saline (PBS) for 5 min. Later, the brain sections were incubated with 0.3 % thioflavin S (Sigma-Aldrich) for 20 min at room temperature in the dark. Subsequently, these were submitted to washes in 3-min series, specifically with 80 % ethanol (two washes), 90 % ethanol (one wash), and three washes with PBS. Finally, the slides were mounted using Fluoromount (EMS), allowed to dry overnight at room temperature in the dark, and stored at 4 °C. Image acquisition was performed with an epifluorescence microscope (BX41; Olympus, Germany). For plaque quantification, similar and comparable histological areas were selected, focusing on having the hippocampus and the whole cortical area positioned adjacently.

Quantification of soluble β-amyloid

Frozen samples of the cortex and hippocampus of SHAP(+), SHAP(−), APP/PS1, and SAMP8 mice aged 3, 6, 9, and 12 months were wet mass determined (120 mg) and homogenized in ice-cold guanidine buffer (5 M guanidine hydrochloride/50 mM Tris-Cl, pH 8.0). The detection and measurement of β-amyloid 1-40 and β-amyloid 1-42 was carried out by enzyme-linked immunoabsorbent assay (ELISA) with the corresponding detection kits (Invitrogen, Carlsbad, CA, USA), following the instructions of the supplier and after optimizing the reaction with increasing amounts of known concentrations of β-amyloid 1-40 and β-amyloid 1-42.

Immunohistochemistry

Slides were allowed to defreeze at room temperature and then rehydrated with PBS for 5 min. Then, brain sections were blocked and permeabilized with PBS containing 1 % bovine serum albumin (BSA; Sigma-Aldrich) and 0.1 % Triton X-100 (Sigma-Aldrich) for 20 min. After two, 5-min washes in PBS, the slides were incubated with the primary antibody for Iba-1 (WAKO, 1:500) and glial fibrillary acidic protein (GFAP, Abcam, 1:500) (see Table 1) overnight at 4 °C. They were then washed again and incubated for 1 h at room temperature in the dark with Alexa Fluor secondary antibody. Finally, the slides were washed, mounted using Fluoromount (EMS), allowed to dry overnight at room temperature, and stored at 4 °C. Image acquisition was performed with an epifluorescence microscope (BX41, Olympus, Germany).

Table 1

List of antibodies used

Primary antibody	Host	Source	Catalog	Work dilution	
				IHC	WB
APP C-terminal	Mouse	Covance	SIG-39152		1:1000

Primary antibody	Host	Source	Catalog	Work dilution	
				IHC	WB
BACE1	Rabbit	Millipore	AB5832		1:500
CDK5	Rabbit	Santa Cruz Biotech	sc-173		1:1000
ERK-1/2	Rabbit	Cell Signaling	#9102		1:1000
GSK3β	Rabbit	Cell Signaling	#9315		1:1000
p35/p25	Rabbit	Cell Signaling	#2680		1:1000
Phospho-Tau Ser199	Rabbit	Invitrogen	44734G		1:1000
Phospho-Tau Tyr205	Rabbit	Invitrogen	44738G		1:1000
Phospho-Tau Ser396	Rabbit	Invitrogen	44752G		1:1000
Phospho-Tau Ser404	Rabbit	Invitrogen	44758G		1:1000
Phospho-ERK-1/2 (Thr202/Tyr204)	Rabbit	Cell Signaling	#9101		1:1000
Phospho-GSK3β (P-Tyr216)	Rabbit	Abcam	ab75745		1:1000
Phospho-SapK/JNK (Thr183/Tyr185)	Mouse	Cell Signaling	#9255		1:2000
Presenilin 1	Rabbit	Calbiochem	529592		1:1000
SapK/JNK	Rabbit	Cell Signaling	#9252		1:1000
Total tau	Mouse	Abcam	ab39524		1:500
β-Actin	Mouse	Sigma-Aldrich	A5441		1:20,000
Alexa Fluor 488 donkey anti-mouse IgG A				1:50	
Alexa Fluor 546 donkey anti-rabbit IgG A				1:50	
Iba-1	Rabbit	Wako Chemicals	019-19741	1:250	
GFAP	Mouse	Abcam	ab10062	1:250	

Open in a separate window

IHC immunohistochemistry, *WB* Western blot

Protein extraction

Brains were micronized by freezing with liquid nitrogen and grinding with a mortar. For total protein extraction, lysis buffer (50 mM Tris-HCl, 150 mM NaCl, 5 mM EDTA, 1 % Triton X-100, pH 7.4), EDTA-free protease inhibitor cocktail (Roche, Mannheim, Germany), and phosphatase inhibitor cocktail 1 (Sigma-Aldrich, St. Louis, MO, USA) were added to the micronized tissue and left on ice for 30 min. Then, the samples were centrifuged at 10,000 × *g* for 10 min and a supernatant with total protein content was collected. All of the protein extraction steps were carried out at 4 °C. Protein concentration was determined by the Bradford protein assay.

Western blot

For Western blot analysis, 20 μg of protein was denatured at 95 °C for 5 min in sample buffer (0.5 M Tris-HCl, pH 6.8, 10 % glycerol, 2 % sodium dodecyl sulfate (SDS), 5 % β-mercaptoethanol, 0.05 % bromophenol blue), separated by sodium dodecyl sulfate-polyacrylamide gel electrophoresis (SDS-PAGE) onto 8–12 % polyacrylamide gels and transferred onto Immobilon polyvinylidene difluoride membranes (Millipore, Billerica, MA, USA). The membranes were incubated overnight at 4 °C with the primary antibodies (see Table 1) diluted with Tris-buffered saline containing 0.1 % Tween 20 (TBS-T) and 5 % BSA. Membranes were then washed and incubated with secondary antibodies (see Table 1) and diluted with TBS-T for 1 h at room temperature. Protein bands were visualized using a

chemiluminescent HRP substrate (Millipore) and ChemiDoc XRS+ (Bio-Rad). Band intensities were quantified by densitometric analysis using Image Lab software and values were normalized to β-actin, except for C-terminal fragments (CTF) of APP (14 kDa), also named C99, which were normalized by APP protein and phospho-tau protein levels, which were normalized by total tau protein.

Statistical analysis

Results were analyzed statistically by SPSS 19.0 (SPSS Inc., Chicago, IL, USA) software and GraphPad PRISM (GraphPad Software, Inc.) software. Data are presented as mean ± standard error of the mean (SEM), and means were compared with two-tailed, unpaired Student *t* test or one-way analysis of variance (ANOVA) followed by Tukey's multiple comparison test when necessary. In the ORT, a one-sample *t* test was used to examine whether single columns were different from zero. Statistical significance was attained when *p* values were <0.05.

Results

Go to:

SHAP mice characteristics across aging

Throughout the study, animal weight monitoring was conducted weekly. From the results (Fig. 1), it can be observed that at early ages, weights of the novel mice obtained did not show significant weight differences among themselves but did in comparison with parental strains APP/PS1 and SAMP8. When age and differences among strains were maintained and weight gain patterns were similar in SHAP and APP/PS1 model, increasing over time, in turn and as expected, SAMP8 presented a very weak growth, with significantly lower weight than other experimental groups.

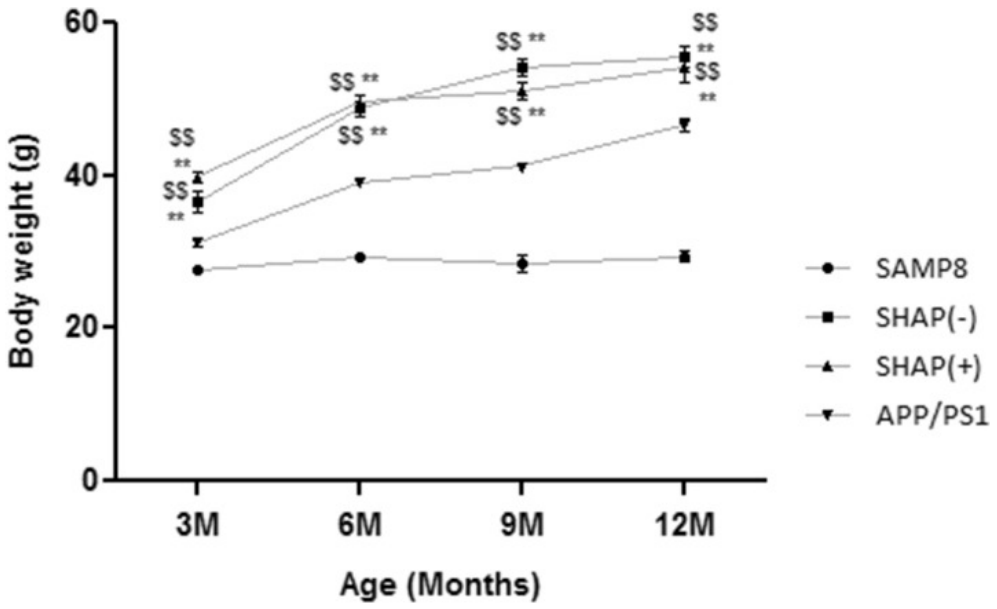

Fig. 1

Body weight (BW, in grams [g]) of the studied models in function of age (months). Analysis of variance (ANOVA) following Tukey's multiple comparison test: $^{**}p < 0.01$ vs. SAMP8; $^{\$\$}p < 0.01$ vs. amyloid precursor protein/presenilin 1 (*APP/PS1*)

Object recognition test

At late age (9 and 12 months), ORT demonstrated that SAMP8, APP/PS1, and SHAP(+) mice showed impaired memory, while SHAP(−) did not (Fig. 2). To date, it has been found that transgenic mice with

SHAP(+) maintain loss of memory, but preservation of memory in comparison with SAMP8 occurs when transgenes are not present in SHAP(−) mice.

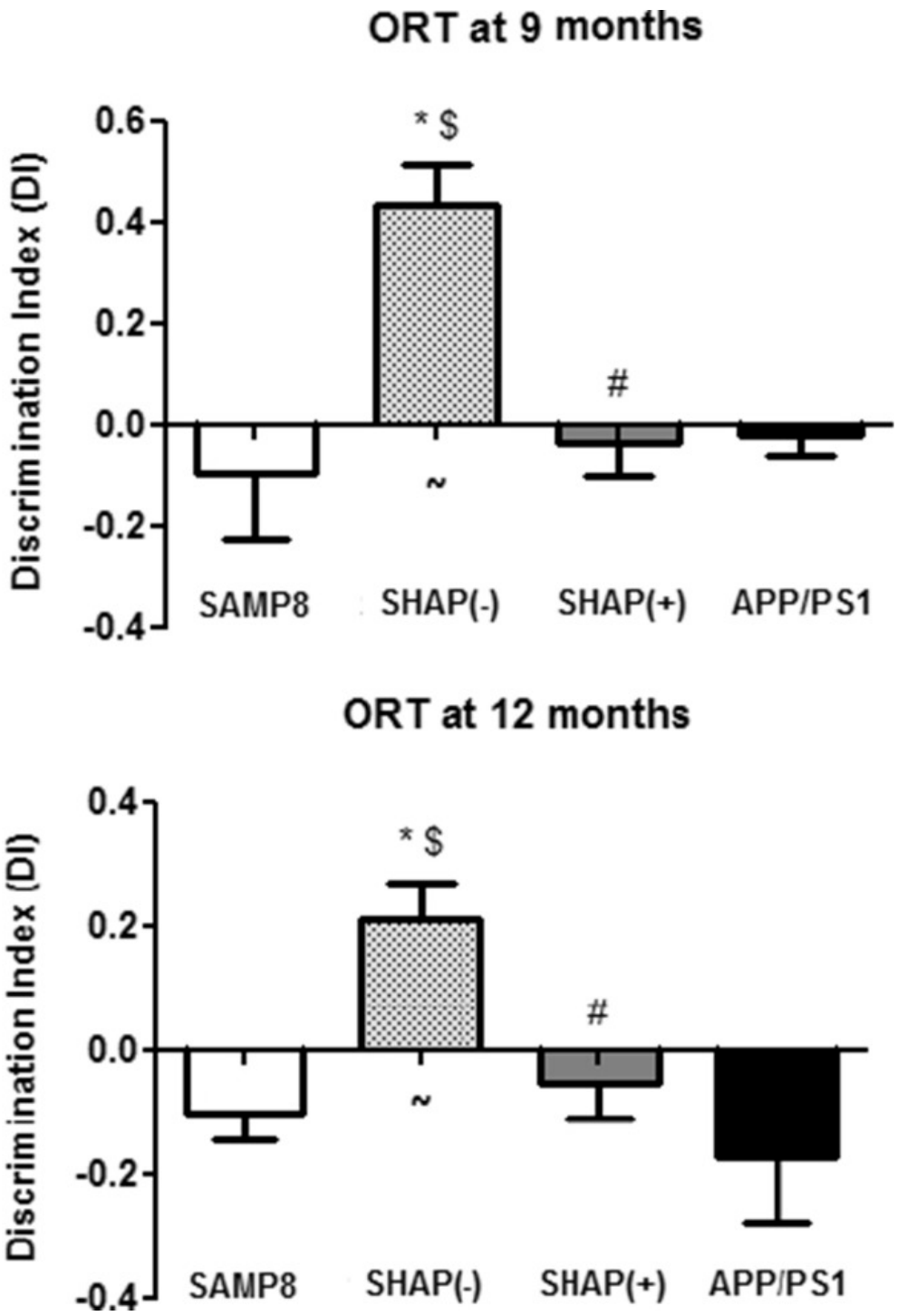

Open in a separate window

Fig. 2

Discrimination index (*DI*) of different groups of senescence-accelerated mouse prone 8 (*SAMP8*) animals at 9 and 12 months of age. *Bars* represent mean ± standard error of the mean (SEM). Analysis of variance (ANOVA) following Tukey's multiple comparison test: one-sample *t* test—*$p < 0.05$ vs. SAMP8; $^{\$}$ $p < 0.05$ vs. APP/PS1; $^{\#}$ $p < 0.05$ vs. SHAP(−)

Histopathologic brain state

Plaque histopathologic state was analyzed in all experimental groups and at each age through thioflavin S staining. No SP were determined in any mouse strains at 3 months (data not shown), as described previously for APP/PS1 and SAMP8 mice (Butterfield and Poon 2005; Aso et al. 2012). Strains expressing APP and PS1 transgenes showed a burden of Aβ depositions that increased with age (Fig. 3g–l), whereas SAMP8 and SHAP(−) strains, both without transgene, did not (Fig. 3a–f). Specifically, APP/PS1 showed early deposition at 6 months (Fig. 3j), always exhibiting higher levels of Aβ deposition in the cortex than in hippocampus areas (Fig. 4). Conversely, SHAP(+) mice demonstrated a delayed initial deposition time. At 9 months, SHAP(+) presented SP (Fig. 3h) and displayed higher levels in comparison with APP/PS1 at this age (Figs. 3k and 4a). At 12 months, SHAP(+) showed increased levels of burden Aβ deposition in all studied areas (Figs. 3i–l and 4a), in comparison with APP/PS1 (Figs. 3l and 4l). We found significant higher soluble Aβ-40/42 levels in both transgenic strains in reference to SAMP8 and SHAP(−) (Fig. 4b, c). Increasing quantities of soluble Aβ-42 were determined in SHAP(+) in front of APP/PS1, only at 3-months old.

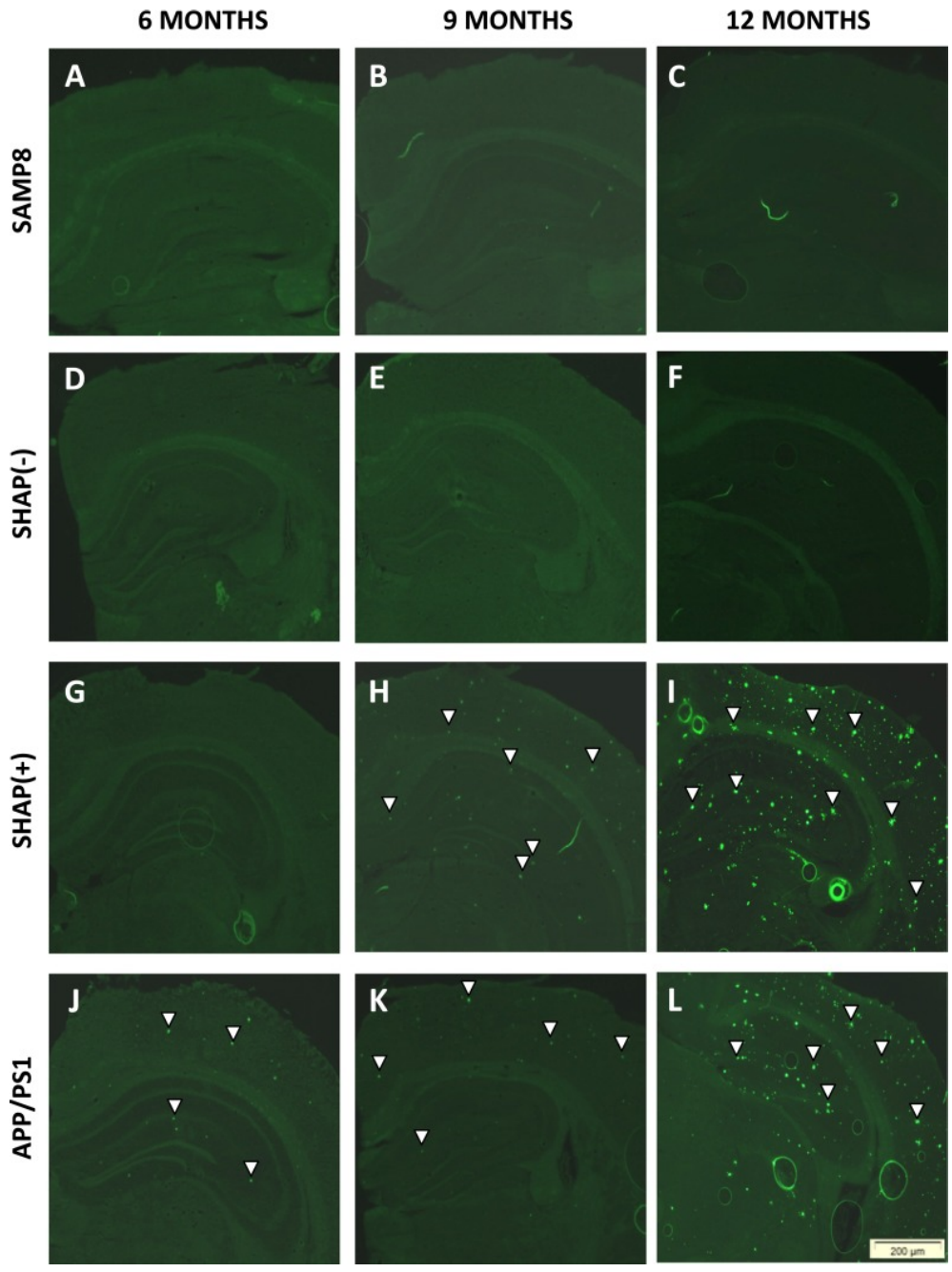

Open in a separate window

Fig. 3

Thioflavin S staining of β-amyloid plaques in mouse brains. Representative images of histopathological brain state of senescence-accelerated mouse prone 8 (*SAMP8*) (**a**–**c**), SHAP(+) (**d**–**f**), SHAP(−) (**g**–**i**), and amyloid precursor protein/presenilin 1 (*APP*/*PS1*) (**j**–**l**) at different times in life (6, 9, and 12 months). *White arrows* are representative indicators of the presence of β-amyloid plaques in the areas studied: cortex (Cx) and hippocampus (Hp)

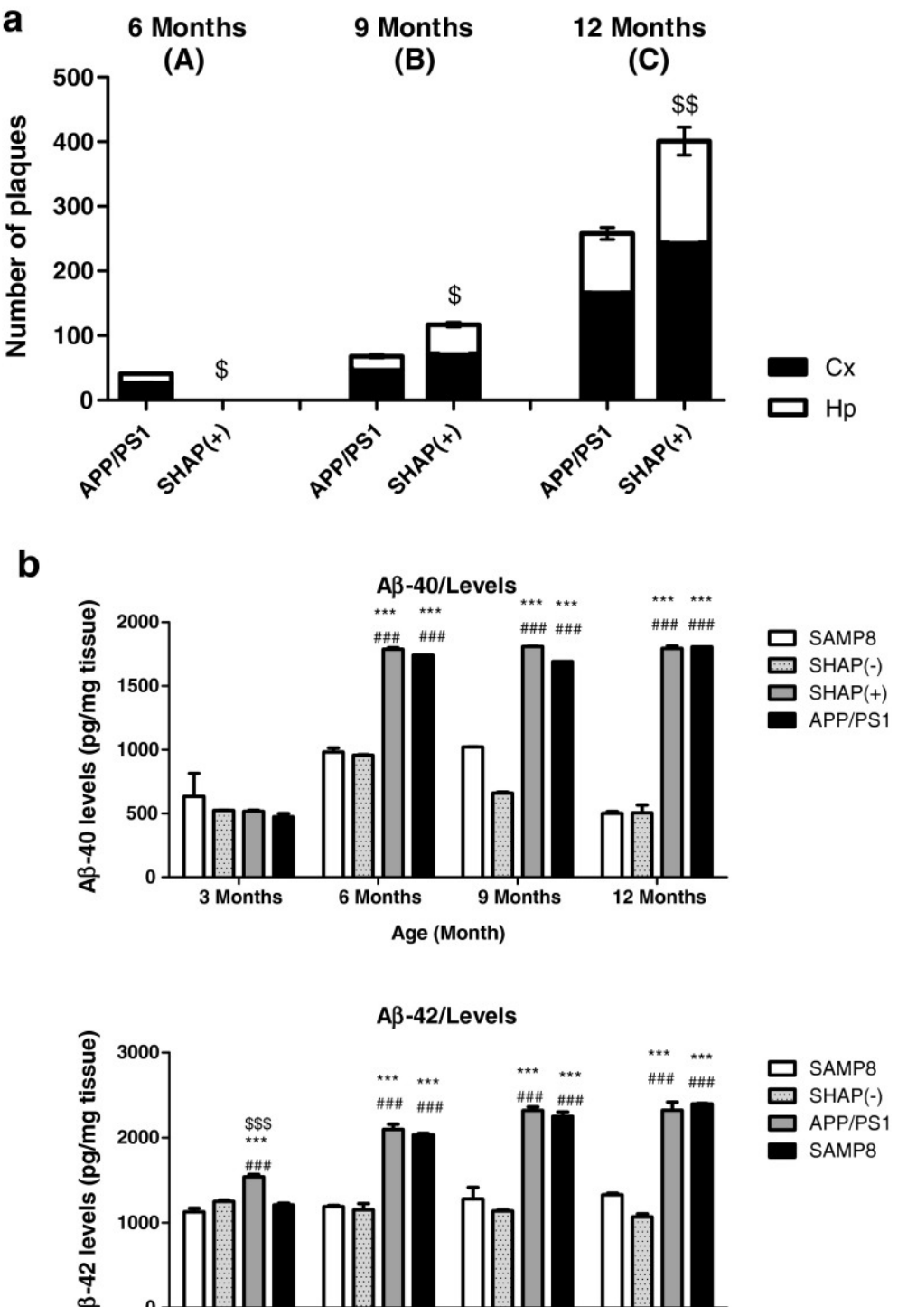

Open in a separate window

Fig. 4

a Quantification of number of β-amyloid plaques at 6, 9, and 12 months of age in the cerebral cortex (*Cx*) and hippocampus (*Hp*) of amyloid precursor protein/presenilin 1 (*APP/PS1*) and SHAP(+). **b** Levels of soluble Aβ-40 and Aβ-42, respectively, at 3, 6, 9, and 12 months. For quantification parameters, see "Materials and methods." *Bars* represent mean ± standard error of the mean (SEM). Analysis of variance (ANOVA) following Tukey's multiple comparison test: ***$p < 0.001$ vs. SAMP8 and SHAP(−); $^{\$}$ $p < 0.05$, $^{\$\$}$ $p < 0.01$, $^{\$\$\$}$ $p < 0.001$ vs. APP/PS1, $^{\#\#\#}$ $p < 0.001$

Gliosis, linked with SP formation, was assessed by GFAP immunohistochemistry at the final stage (12 months). Results showed astroglial activation in APP/PS1 (Fig. 5n, p) and SHAP(+) (Fig. 5j, l) but not in SAMP8 (Fig. 5b, d) and SHAP(−) (Fig. 5f, h). Double staining with thioflavin S and GFAP demonstrated the colocalization of astroglial reactivity with β-amyloid deposition in APP/PS1 and SHAP(+), confirming that glial activation is related with the presence of amyloid protein aggregates both in cortical (Fig. 5j, n) and hippocampal areas (Fig. 5l and p). Conversely, when microglial activation was determined by Iba-1 immunohistochemistry, mice with APP/PS1 double transgene, SHAP(+), and APP/PS1 exhibited some degree of microglial activation in cortical regions (Fig. 5i and m) and the hippocampus (Fig. 5k and o).

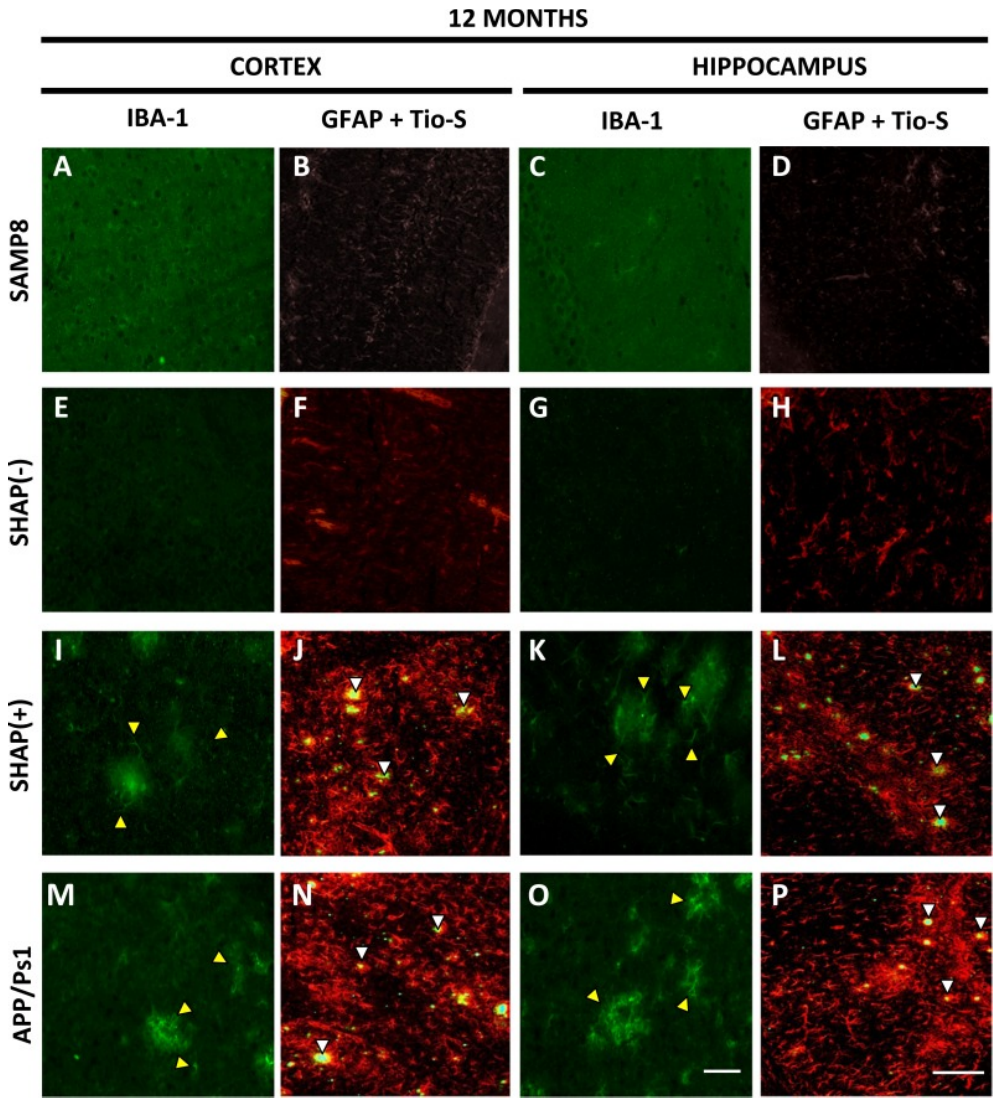

Open in a separate window

Fig. 5

Immunohistochemical (cortex and hippocampus) staining of Iba-1 (*green*) and GFAP (*red*). Representative images of glial state of senescence-accelerated mouse prone 8 (*SAMP8*) (**a**–**d**), SHAP(+) (**i**–**l**), SHAP(−) (**e**–**h**), and amyloid precursor protein/presenilin 1 (*APP*/*PS1*) (**m**–**p**) mice at 12 months of age. *Yellow arrows* are representative indicators of microglial activation in studied areas, whereas *white arrows* are representative indicators of β-amyloid plaques and glial fibrillary acidic protein (*GFAP*) staining. *Scale bar* for Iba-1 images is 100 μm, for GFAP + Tio-S 200 μm

Amyloid pathology in the APP/PS1/SAMP8

On observing changes in β-amyloid deposition in the newly generated strain, we decided to assess the effect of age on the level of β-secretase (BACE1), PS1, and known intermediates and end products of APP processing.

Highest levels in BACE1 were found in SAMP8 and in newly generated mice SHAP(+) and SHAP(−) in reference to APP/PS1 at up to 9 months (Fig. 6). In contrast, at 12 months, APP/PS1 achieved the highest levels of BACE1 compared with SAMP8 and SHAP mice (Fig. 6). An increase in 48 kDa fragment, corresponding to the catalytic core of PS1, was detected only in SHAP(+) at the oldest age

tested (12 months) (Fig. 7). In reference to the proteolytic fragment (18 kDa) of constitutive PS1, we determined a higher level in SAMP8 in reference to mice carrying the human PS1 mutation, APP/PS1, and SHAP(+) according to the nature of this mutation (Fig. 6), which do not require cleavage activation of PS1, being constitutively active. Surprisingly, APP/PS1 exhibited an increase in this fragment at 12 months, indicating possible endoproteolysis of the endogenous murine PS1 isoform.

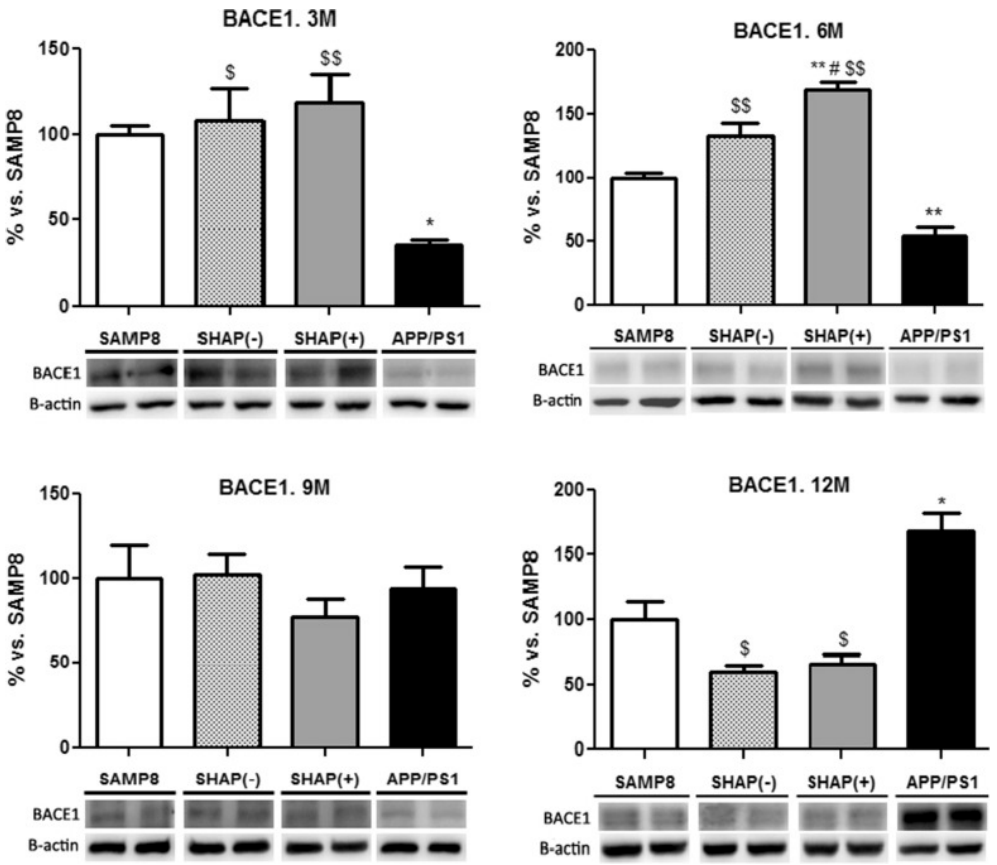

Fig. 6

Levels of BACE of senescence-accelerated mouse prone 8 (*SAMP8*), SHAP(−), SHAP(+), and amyloid precursor protein/presenilin 1 (*APP*/*PS1*). *Bars* represent mean ± standard error of the mean (SEM); values are adjusted to 100 % for levels of SAMP8. Analysis of variance (ANOVA) following Tukey's multiple comparison test: $*p < 0.05$, $**p < 0.01$ vs. SAMP8; $^{\$}\ p < 0.05$, $^{\$\$}\ p < 0.01$ vs. APP/PS1; $^{\#}\ p < 0.05$ vs. SHAP(−)

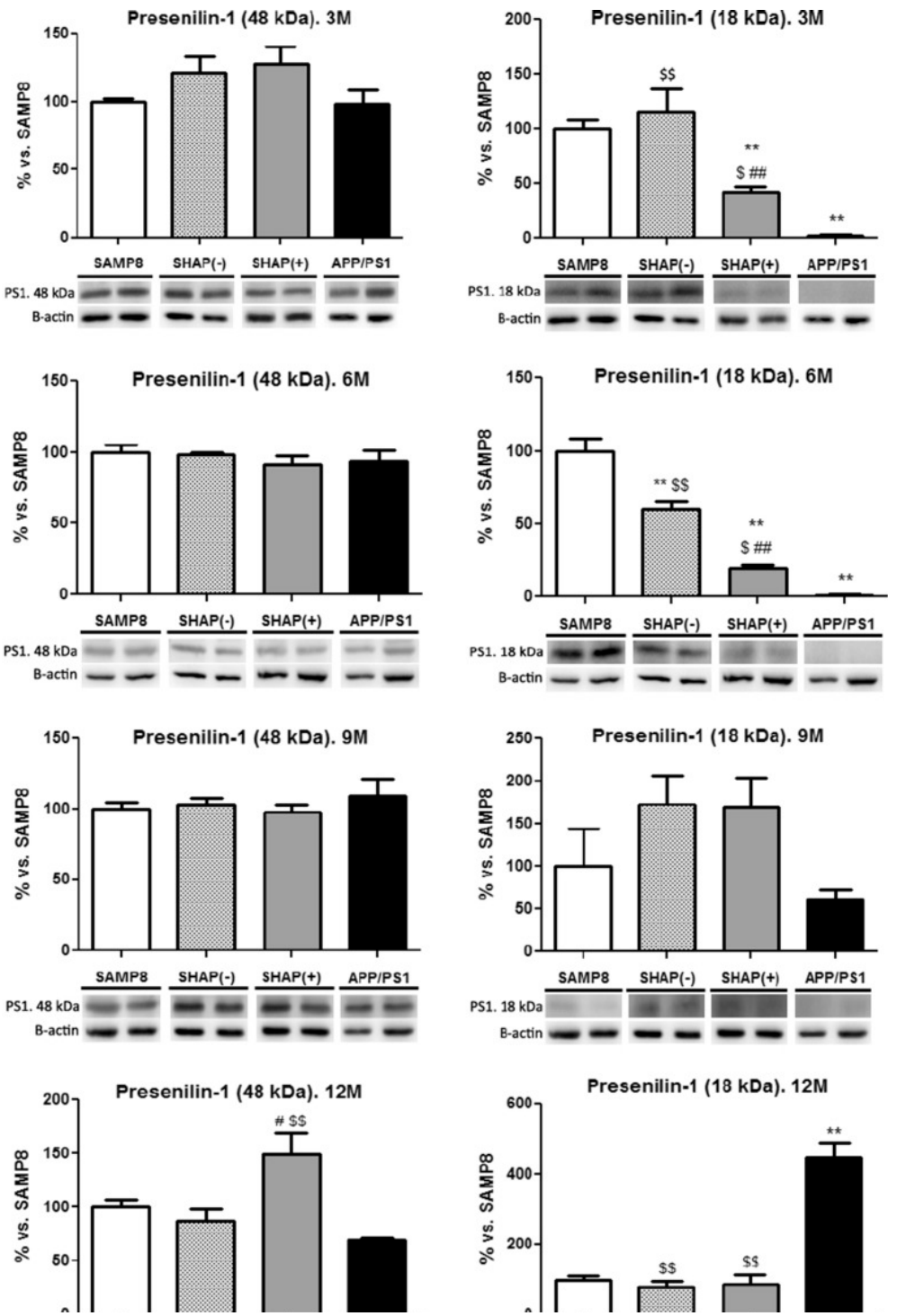

Open in a separate window

Fig. 7

Levels of presenilin 1 (*PS1*), holoprotein (48 kDa), and CTF fragment (18 kDa) of senescence-accelerated mouse prone 8 (*SAMP8*), SHAP(−), SHAP(+), and amyloid precursor protein/presenilin 1 (APP/PS1) mice. *Bars* represent mean ± standard error of the mean (SEM); values are adjusted to 100 % for levels of SAMP8. Analysis of variance (ANOVA) following Tukey's multiple comparison test: $^{**}p < 0.01$ vs. SAMP8; $^{\$}p < 0.05$, $^{\$\$}p < 0.01$ vs. APP/PS1; $^{\#}p < 0.05$, $^{\#\#}p < 0.01$ vs. SHAP(−)

Levels of APP and C99 fragment were significantly increased in SHAP(+) and APP/PS1 in comparison with SHAP(−) and SAMP8 mice aged 3 and 6 months, respectively (Fig. 8). These facts are in agreement with the presence of the APP transgene and higher Aβ deposition in these mice but not in SHAP(−) and SAMP8.

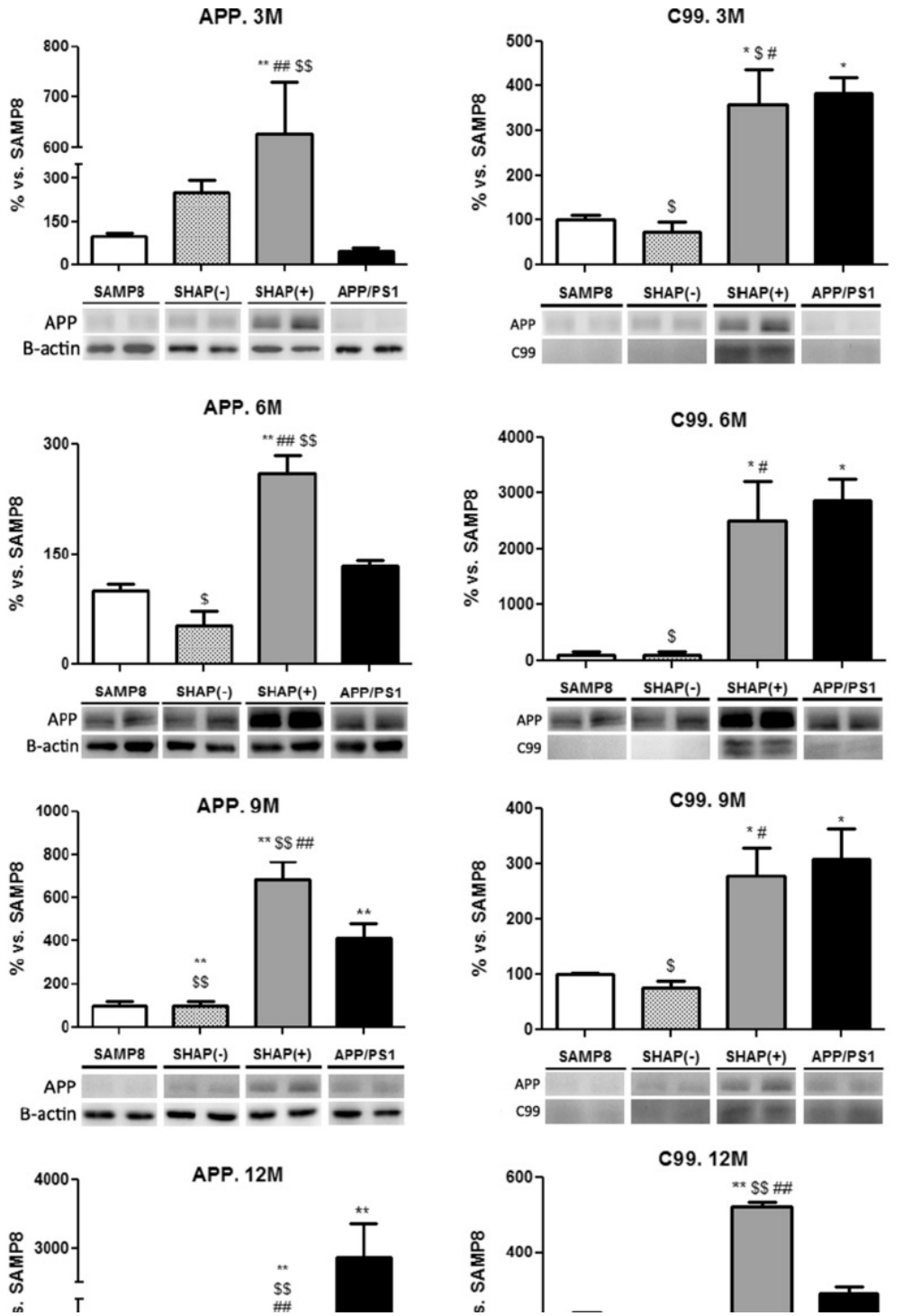

Open in a separate window

Fig. 8

Western blot analysis for amyloid precursor protein (*APP*) of senescence-accelerated mouse prone 8 (SAMP8), SHAP(−), SHAP(+), and APP/presenilin 1 (PS1) mice. *Upper panels* present the analysis of

full APP levels at the studied ages. *Lower panels* present C-terminal beta fragment (CTFß/APP ratio). *Bars* represent mean ± standard error of the mean (SEM); values are adjusted to 100 % for levels of SAMP8. Analysis of variance (ANOVA) following Tukey's multiple comparison test: $*p < 0.05$, $**p < 0.01$ vs. SAMP8; $^{\$}p < 0.05$, $^{\$\$}p < 0.01$ vs. APP/PS1; $^{\#}p < 0.05$, $^{\#\#}p < 0.01$ vs. SHAP(−)

Characterization in tau pathology

Different tau phosphoepitopes were studied, including Tau Ser199, Tau Tyr205, Tau Ser396, and Tau Ser404. Along the aging process studied in this novel strain, no changes were observed in the levels of the different phospho-tau studied, which presented high variability in the levels of each epitopes studied, except for APP/PS1 at the oldest age tested, where we observed higher levels of phospho-tau in comparison to SAMP8 (Fig. 9). In addition, we studied total tau levels along the aging process, and it did not show significant changes in these levels (data not shown).

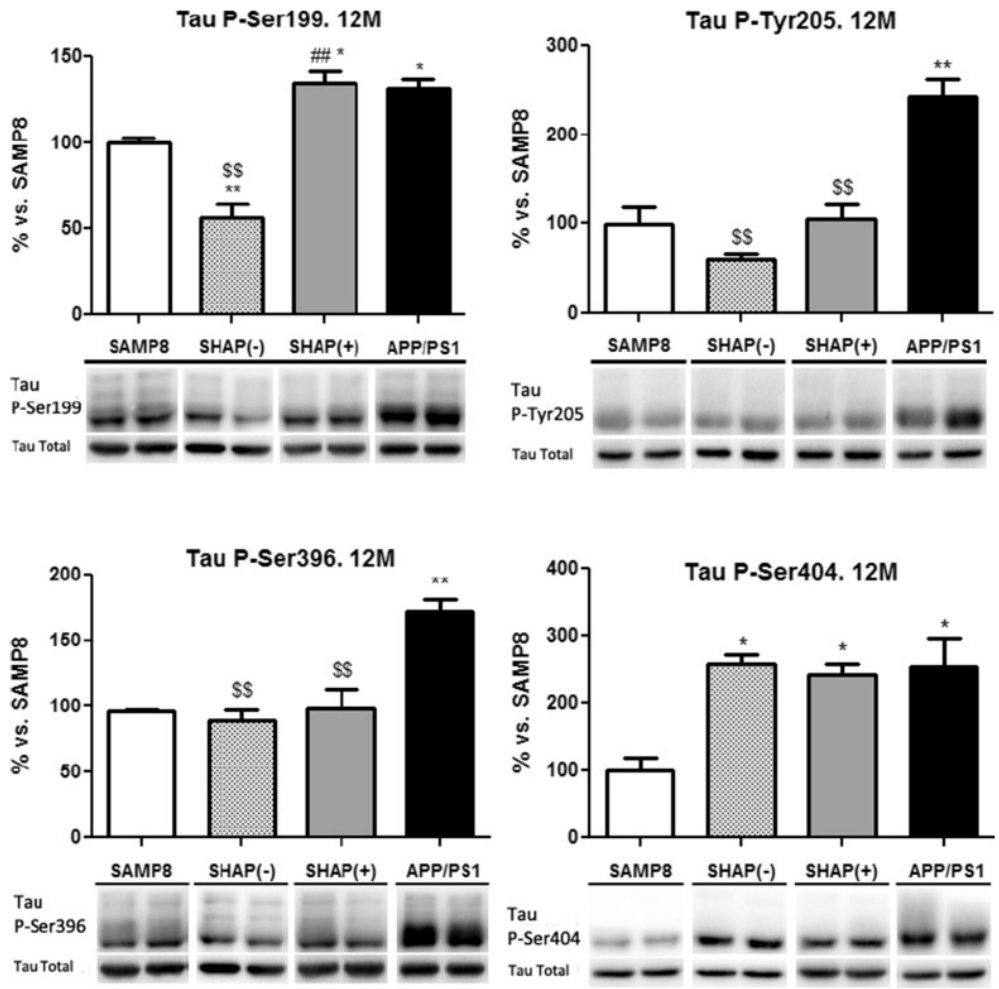

Fig. 9

Levels of phosphorylated Tau at Ser199, Tyr205, Ser396, and Ser404 epitopes. *Bars* represent mean ± standard error of the mean (SEM) and values are adjusted to 100 % for levels of senescence-accelerated mouse prone 8 (*SAMP8*) mice. Analysis of variance (ANOVA) following Tukey's multiple comparison test: $*p < 0.05$, $**p < 0.01$ vs. SAMP8; $^{\$\$}p < 0.01$ vs. APP/PS1; $^{\#}p < 0.05$, $^{\#\#}p < 0.01$ vs. SHAP(−)

GSK3β (phospho-Tyr279) levels, the active forms of these tau kinases, were higher in SHAP(+) than in APP/PS1 and SAMP8 (Fig. 10). At the same time, higher levels of CDK5 were determined in SHAP(+) at 12 months in comparison with SAMP8 and APP/PS1, concurrently with an increase in the coactivator p25, indicating a possible enhanced process of phosphorylation in these animals (Figs. 9 and 10). Also, phospho-SapK/c-Jun N-terminal kinase (JNK) was raised in SHAP(+) in comparison with reference to SAMP8 and APP/PS1 (Fig. 10).

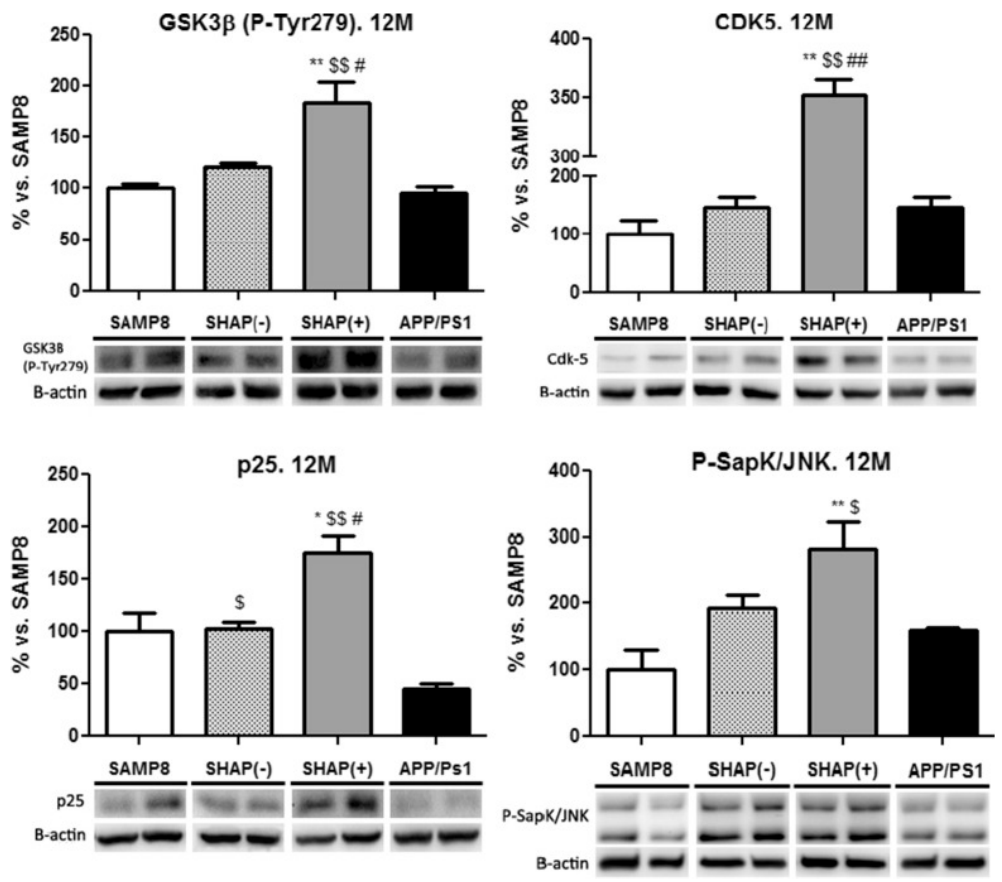

Fig. 10

Levels of CDK5, p25, GSK3β, and SAPK/JNK. *Bars* represent mean ± standard error of the mean (SEM) and values are adjusted to 100 % for levels of senescence-accelerated mouse prone 8 (*SAMP8*) mice. Analysis of variance (ANOVA) following Tukey's multiple comparison test: $*p < 0.05$, $**p < 0.01$ vs. senescence-accelerated mouse prone 8 (SAMP8); $^{\$}p < 0.05$, $^{\$\$}p < 0.01$ vs. amyloid precursor protein/presenilin 1 (*APP*/*PS1*); $^{\#}p < 0.05$, $^{\#\#}p < 0.01$ vs. SHAP(−)

Oxidative enzymatic machinery

Levels of SOD1, catalase, and iNOS were determined by Western blot to detect changes in the oxidative machinery in the new generated strain, that is SHAP(+). Results showed no changes in any of the enzymes linked with oxidative stress (OS) (data not shown).

Discussion

Go to:

Current mouse models of AD are restricted to the expression of AD-related pathology associated with specific mutations present in early-onset fAD, thus representing <5 % of AD cases. To date, there are no mouse lines that model continuum development and late-onset/age-related AD, which accounts for the

vast majority; therefore, the chronology of events that lead to the disease in the aged population is difficult to establish based on current animal models. Moreover, published data show that SAMP8, a model of accelerated aging, displays many features in the brain that are known to occur in AD (i.e., increased OS, Aβ alterations, and tau hyperphosphorylation) (Takeda 2009; Morley et al. 2012). Therefore, SAMP8 mice may offer an excellent model for studying the earliest neurodegenerative changes associated with AD and provide a more encompassing picture of the disease, considering AD as a syndrome triggered by a combination of age-related events. On the other hand, APP/PS1 are double transgenic mice that express a chimeric mouse/human amyloid precursor protein (Mo/HuAPP695swe) and a mutant human presenilin 1 (PS1-ΔE9). The presence of amyloid burden in the cortex and hippocampus (CA3 and CA1) were demonstrated in APP/PS1 transgenic mice available at our laboratory (Aso et al. 2012). To date, the leading hypothesis, the Aβ hypothesis, which is based on mutations in either APP or PS1/2 that affect the processing of APP and contribute to Aβ accumulation in neurons and to the consequent formation of senile plaques (Perry et al. 2000), has come under increased scrutiny. In fact, it is becoming increasingly discussed that Aβ deposition could be a consequence, rather than an initiator, of the pathophysiological cascade (Swomley et al. 2013). Other mechanisms of the disease, such as abnormally hyperphosphorylated bundles of tau protein found in neurofibrillary tangles, oxidative stress, metal ion deregulation, inflammation, and age, must be taken into account in order to delineate the complete picture of the disease (Verri et al. 2012; Swomley et al. 2013).

Recently, Lok et al. (2013a, b) crossed APP/PS1 mice with the SAMP8 generating a new AD mouse model, expressing human APP/PS1 genes on a senescence background, covering a phenotypical analysis by studying working memory, spatial memory, motor performance, and anxiety-like behavior, as well as changes in neuronal cell death and amyloid deposition. We applied the same strategy in the present work, crossing APP/PS1 with SAMP8, delivering a double transgenic mouse in SAMP8 background, named SHAP(+). The goal was to better characterize at the biochemical and molecular levels in this mouse with neuropathological traits of human AD in a senescence environment. Both short- and long-term memory deficits are hallmarks of AD. While long-term memory impairment appears only when the disease is in advanced stages and usually already diagnosed, early stages of the disease are characterized by short-term memory deficits (Grady 2001) and they have been widely used as an indicator of AD onset. Thus, only short-term memory deficits were assessed in this study, showing that SHAP(+) had similar memory disturbances to those of SAMP8 and APP/PS1 at old ages, in accordance with impairment in spatial memory or working memory reported earlier (Lok et al. 2013a, b). Short-term memory loss was accompanied by a significant increase in SP, these being the highest at 12 months of age compared with SAMP8 and APP/PS1.

The Swedish mutations (K595N/M596L) included increased the amount of Aβ produced by favoring the processing through the secretase pathway. Levels of APP were higher in SHAP(+) in mice aged up to 9 months old, probably related with SAMP8 strain (Kumar et al. 2009), but at 12 months, these were lower than in APP/PS1, probably due to higher cleavage to the amyloid peptides that accumulate in the plaques that, as previously mentioned, were significantly increased at this stage. Analysis of BACE1, a β-secretase, revealed that there were sparse and no consistent changes in SHAP(+) in comparison to SAMP8. In SAMP8 and SHAP(−), where the transgenic mutant human presenilin protein (PS1-ΔE9) and human APP were not expressed, there were no amyloid depositions; therefore, the expression of human PS1 and APP in APP/PS1 in SHAP(+) is the key factor for amyloid accumulation in these two strains, to a greater degree than the presence and levels of BACE1.

In reference to PS1 function, it is known that uncleaved PS1 holoprotein (full-length PS) (48–52 kDa) is an inactive zymogene that must be activated by endoproteolytic cleavage (Li et al. 2000; Fukumori et al. 2010). There is compelling evidence that full-length PS1 is subject to endoproteolytic processing, generating N-terminal (NTF) (27–28 kDa) and CTF (16–18 kDa) (Thinakaran et al. 1996; Chávez-Gutiérrez et al. 2008). Once PS1 is cleaved, NTF (27–28 kDa) and CTF (16–18 kDa) form a biologically active NTF-CTF heterodimer, and the γ-secretase substrate can reach the catalytic site (Chávez-Gutiérrez et al. 2008; Ahn et al. 2010; Wolfe 2013). Removal of exon 9 in the PS1-ΔE9

mutation allows access to the catalytic site, resulting in the constitutively active form of the enzyme as holoprotein, without the need for the cleavage process (Knappenberger et al. 2004). Accordingly, we found higher levels of active fragment in SAMP8 and SHAP(−) mice than in mice supporting the mutation, at early ages. However, levels of 18 kDa PS1 normalized with age. In contrast, holoprotein PS1 levels were similar in all experimental groups up to the age of 9 months but were found significantly increased in SHAP(+) at 12 months of age in comparison with APP/PS1, in agreement with higher Aβ deposition in these mice at the same age. The greater participation of PS1 in amyloid pathology, described in APP/PS1 and in SHAP(+), would be of importance when new drugs are studied for AD treatment, and that it will be more interesting to focus on PS1 inhibitors rather than on BACE inhibitors (Gandy and DeKosky 2013).

Increases in tau hyperphosphorylation also participate in exacerbating plaque formation; thus, the presence of higher hyperphosphorylation processes could be the cause of the increase in amyloid pathology (Guo et al. 2013). Therefore, to determine a possible link between amyloidosis and tau pathology in SHAP(+) mice, we studied tau phosphorylation in several characteristic serine and tyrosine epitopes in these mice in comparison with SAMP8 and APP/PS1. As described elsewhere, both SAMP8 and APP/PS1 possess an alteration in the tau phosphorylation process (Canudas et al. 2005; Aso et al. 2012). Total tau content was raised in APP/PS1 in comparison with that of SAMP8, whereas in SHAP(+) levels, tau content was nearer to that of the senescence model (data not shown). Four different phosphorylated epitopes were studied here. No changes were found and there is no clear correlation between phosphorylation levels and the mouse strain at early and medium age. At 12 months, the oldest age studied, APP/PS1 and SHAP(+) exhibited higher phosphorylation in Tau Ser199, Tau Ser396, and Tau Ser404. Moreover, the data showed no specific correlation between tau and amyloid pathology up to 12 months, where amyloid pathology was well established, as our results and the broad bibliography published on APP/PS1 or in SAMP8 demonstrate (Lok et al. 2013a, b).

The lack of difference in phosphorylated tau epitope patterns studied in early ages among the strains is in agreement with the no differential activation of tau kinases CDK5 and GSK3β until 9 months, at least in SHAP(+). Instead, at 9 and at 12 months, SHAP(+) displayed an altered kinase pattern that correlates with tau hyperphosphorylation, which shows higher phosphorylation levels in Ser199 and Ser404 epitopes. This fact is in agreement with the literature, which describes tau as a substrate for CDK5 and GSK3β (Iqbal and Grundke-Iqbal 2008; Casadesús et al. 2012). In turn, this pattern also correlates with the overexpression of CDK5 and p25, which results in increased tau phosphorylation at specific sites (Currais et al. 2013). JNK has been implicated in tau phosphorylation in APP/PS1 and SAMP8 mice (Díaz-Moreno et al. 2013). Levels of JNK are also increased in SHAP(+) at 12 months of age in comparison with SAMP8 or APP/PS1.

OS is a well-established pathogenic factor in AD, and the association of OS with amyloid and tau abnormalities is well known (Mondragón-Rodríguez et al. 2013). A redox imbalance has been described in both SAMP8 and APP/PS1. The newly generated mice, SHAP(+), did not differ in protein levels related with homeostatic control of OS, synch as catalase, superoxide dismutase (SOD), or nitric oxide (NO) synthase. On the other hand, immunohistochemical studies showed that microgliosis and astrogliosis were detectable in APP/PS1 and SHAP(+) in the hippocampus and cortex, indicating that the OS described for APP/PS1 was present also in the SHAP(+). In reference to astrogliosis, and as expected, reactive astroglia are localized near the plaques both in APP/PS1 and SHAP(+), indicating that OS and a harmful effect occur mainly surrounding amyloid aggregation.

Conclusion

Go to:

In conclusion, overexpression of APP and PS1 in a senescence background of SAMP8 generates a model of AD linked with senescence, with exacerbation of the amyloidogenic process at late ages, and maintains some of the histopathological hallmarks present in AD and also learning and memory disturbances expected by the effect of aging and disease.

Acknowledgments

Go to:

This study was funded by grants SAF-2012-39852, SAF2011-23631, and SAF2009-13093 from the Spanish Ministerio de Ciencia e Innovación. We thank Dr. Margaret Ellen Reynolds Adlerof for linguistic and style advice and correction of the manuscript and Ms Mar Morales and Silvia Soriano for their technical aid.

Footnotes

Go to:

D. Porquet and P. Andrés-Benito contributed equally to this work.

References

Go to:

Agarwal A, Saleh RA, Bedaiwy MA. Role of reactive oxygen species in the pathophysiology of human reproduction. Fertil Steril. 2003;79:829–43. doi: 10.1016/S0015-0282(02)04948-8. [PubMed] [Cross Ref]

Ahn K, Shelton CC, Tian Y, et al. Activation and intrinsic gamma-secretase activity of presenilin 1. Proc Natl Acad Sci U S A. 2010;107:21435–40. doi: 10.1073/pnas.1013246107. [PMC free article] [PubMed] [Cross Ref]

Antunes M, Biala G. The novel object recognition memory: neurobiology, test procedure, and its modifications. Cogn Process. 2012;13:93–110. doi: 10.1007/s10339-011-0430-z. [PMC free article] [PubMed] [Cross Ref]

Aso E, Lomoio S, López-González I, et al. Amyloid generation and dysfunctional immunoproteasome activation with disease progression in animal model of familial Alzheimer's disease. Brain Pathol. 2012;22:636–53. doi: 10.1111/j.1750-3639.2011.00560.x. [PubMed] [Cross Ref]

Aubele T, Kaufman R, Montalmant F, Kritzer MF. Effects of gonadectomy and hormone replacement on a spontaneous novel object recognition task in adult male rats. Horm Behav. 2008;54:244–52. doi: 10.1016/j.yhbeh.2008.04.001. [PMC free article] [PubMed] [Cross Ref]

Bahrick LE, Hernandez-Reif M, Pickens JN. The effect of retrieval cues on visual preferences and memory in infancy: evidence for a four-phase attention function. J Exp Child Psychol. 1997;67:1–20. doi: 10.1006/jecp.1997.2399. [PubMed] [Cross Ref]

Bancher C, Brunner C, Lassmann H, et al. Accumulation of abnormally phosphorylated τ precedes the formation of neurofibrillary tangles in Alzheimer's disease. Brain Res. 1989;477:90–99. doi: 10.1016/0006-8993(89)91396-6. [PubMed] [Cross Ref]

Borchelt DR, Thinakaran G, Eckman CB, et al. Familial Alzheimer's disease-linked presenilin 1 variants elevate Abeta1-42/1-40 ratio in vitro and in vivo. Neuron. 1996;17:1005–13. doi: 10.1016/S0896-6273(00)80230-5. [PubMed] [Cross Ref]

Braak H, Braak E. Neuropathological stageing of Alzheimer-related changes. Acta Neuropathol. 1991;82:239–59. doi: 10.1007/BF00308809. [PubMed] [Cross Ref]

Braak H, Braak E. Staging of Alzheimer's disease-related neurofibrillary changes. Neurobiol Aging. 1995;16:271–278. doi: 10.1016/0197-4580(95)00021-6. [PubMed] [Cross Ref]

Braak H, Braak E. Evolution of neuronal changes in the course of Alzheimer's disease. J Neural Transm Suppl. 1998;53:127–40. doi: 10.1007/978-3-7091-6467-9_11. [PubMed] [Cross Ref]

Butterfield DA, Poon HF. The senescence-accelerated prone mouse (SAMP8): a model of age-related cognitive decline with relevance to alterations of the gene expression and protein abnormalities in Alzheimer's disease. Exp Gerontol. 2005;40:774–83. doi: 10.1016/j.exger.2005.05.007. [PubMed] [Cross Ref]

Campion D, Dumanchin C, Hannequin D, et al. Early-onset autosomal dominant Alzheimer disease: prevalence, genetic heterogeneity, and mutation spectrum. Am J Hum Genet. 1999;65:664–70. doi: 10.1086/302553. [PMC free article] [PubMed] [Cross Ref]

Canudas AM, Gutierrez-Cuesta J, Rodríguez MI, et al. Hyperphosphorylation of microtubule-associated protein tau in senescence-accelerated mouse (SAM) Mech Ageing Dev. 2005;126:1300–1304. doi: 10.1016/j.mad.2005.07.008. [PubMed] [Cross Ref]

Casadesús G, Gutierrez-Cuesta J, Lee H-G, et al. Neuronal cell cycle re-entry markers are altered in the senescence accelerated mouse P8 (SAMP8) J Alzheimers Dis. 2012;30:573–83. [PubMed]

Chávez-Gutiérrez L, Tolia A, Maes E, et al. Glu(332) in the Nicastrin ectodomain is essential for

gamma-secretase complex maturation but not for its activity. J Biol Chem. 2008;283:20096–105. doi: 10.1074/jbc.M803040200. [PubMed] [Cross Ref]
Codita A, Winblad B, Mohammed AH. Of mice and men: more neurobiology in dementia. Curr Opin Psychiatry. 2006;19:555–63. doi: 10.1097/01.yco.0000245757.06374.6a. [PubMed] [Cross Ref]
Currais A, Prior M, Dargusch R, et al. Modulation of p25 and inflammatory pathways by fisetin maintains cognitive function in Alzheimer's disease transgenic mice. Aging Cell. 2013 [PMC free article] [PubMed]
Del Valle J, Duran-Vilaregut J, Manich G, et al. Early amyloid accumulation in the hippocampus of SAMP8 mice. J Alzheimers Dis. 2010;19:1303–15. [PubMed]
Del Valle J, Duran-Vilaregut J, Manich G, et al. Cerebral amyloid angiopathy, blood-brain barrier disruption and amyloid accumulation in SAMP8 mice. Neurodegener Dis. 2011;8:421–9. doi: 10.1159/000324757. [PubMed] [Cross Ref]
Dewachter I, van Dorpe J, Spittaels K, et al. Modeling Alzheimer's disease in transgenic mice: effect of age and of presenilin1 on amyloid biochemistry and pathology in APP/London mice. Exp Gerontol. 2000;35:831–841. doi: 10.1016/S0531-5565(00)00149-2. [PubMed] [Cross Ref]
Díaz-Moreno M, Hortigüela R, Gonçalves A, et al. Aβ increases neural stem cell activity in senescence-accelerated SAMP8 mice. Neurobiol Aging. 2013;34:2623–38. doi: 10.1016/j.neurobiolaging.2013.05.011. [PubMed] [Cross Ref]
Enserink M. First Alzheimer's diagnosis confirmed. Science. 1998;279:2037. doi: 10.1126/science.279.5359.2037. [PubMed] [Cross Ref]
Feng Y, Wang X. Antioxidant therapies for Alzheimer's disease. Oxid Med Cell Longev. 2012;2012:472932. doi: 10.1155/2012/472932. [PMC free article] [PubMed] [Cross Ref]
Flood JF, Morley JE. Learning and memory in the SAMP8 mouse. Neurosci Biobehav Rev. 1998;22:1–20. doi: 10.1016/S0149-7634(96)00063-2. [PubMed] [Cross Ref]
Fukumori A, Fluhrer R, Steiner H, Haass C. Three-amino acid spacing of presenilin endoproteolysis suggests a general stepwise cleavage of gamma-secretase-mediated intramembrane proteolysis. J Neurosci. 2010;30:7853–62. doi: 10.1523/JNEUROSCI.1443-10.2010. [PubMed] [Cross Ref]
Games D, Adams D, Alessandrini R, et al. Alzheimer-type neuropathology in transgenic mice overexpressing V717F beta-amyloid precursor protein. Nature. 1995;373:523–7. doi: 10.1038/373523a0. [PubMed] [Cross Ref]
Games D, Buttini M, Kobayashi D, et al. Mice as models: transgenic approaches and Alzheimer's disease. J Alzheimers Dis. 2006;9:133–49. [PubMed]
Gandy S, DeKosky ST. Toward the treatment and prevention of Alzheimer's disease: rational strategies and recent progress. Annu Rev Med. 2013;64:367–83. doi: 10.1146/annurev-med-092611-084441. [PMC free article] [PubMed] [Cross Ref]
Glenner GG, Wong CW. Alzheimer's disease and Down's syndrome: sharing of a unique cerebrovascular amyloid fibril protein. Biochem Biophys Res Commun. 1984;122:1131–5. doi: 10.1016/0006-291X(84)91209-9. [PubMed] [Cross Ref]
Grady CL. Altered brain functional connectivity and impaired short-term memory in Alzheimer's disease. Brain. 2001;124:739–756. doi: 10.1093/brain/124.4.739. [PubMed] [Cross Ref]
Guimerà A, Gironès X, Cruz-sánchez FF (2002) Actualización sobre la patología de la enfermedad de Alzheimer. Rev Esp Patol 35:21–48
Guo Q, Li H, Cole AL, et al. Modeling Alzheimer's disease in mouse without mutant protein overexpression: cooperative and independent effects of Aβ and tau. PLoS One. 2013;8:e80706. doi: 10.1371/journal.pone.0080706. [PMC free article] [PubMed] [Cross Ref]
Harvey RJ. The prevalence and causes of dementia in people under the age of 65 years. J Neurol Neurosurg Psychiatry. 2003;74:1206–1209. doi: 10.1136/jnnp.74.9.1206. [PMC free article] [PubMed] [Cross Ref]
Iqbal K, Grundke-Iqbal I. Alzheimer neurofibrillary degeneration: significance, etiopathogenesis, therapeutics and prevention. J Cell Mol Med. 2008;12:38–55. doi: 10.1111/j.1582-4934.2008.00225.x. [PMC free article] [PubMed] [Cross Ref]
Irizarry MC, Soriano F, McNamara M, et al. Abeta deposition is associated with neuropil changes, but not with overt neuronal loss in the human amyloid precursor protein V717F (PDAPP) transgenic

mouse. J Neurosci. 1997;17:7053–7059. [PubMed]
Itzhaki RF. Possible factors in the etiology of Alzheimer's disease. Mol Neurobiol. 1994;9:1–13. doi: 10.1007/BF02816099. [PubMed] [Cross Ref]
Knappenberger KS, Tian G, Ye X, et al. Mechanism of gamma-secretase cleavage activation: is gamma-secretase regulated through autoinhibition involving the presenilin-1 exon 9 loop? Biochemistry. 2004;43:6208–18. doi: 10.1021/bi036072v. [PubMed] [Cross Ref]
Koedam ELGE, Lauffer V, van der Vlies AE, et al. Early- versus late-onset Alzheimer's disease: more than age alone. J Alzheimers Dis. 2010;19:1401–8. [PubMed]
Kumar VB, Franko M, Banks WA, et al. Increase in presenilin 1 (PS1) levels in senescence-accelerated mice (SAMP8) may indirectly impair memory by affecting amyloid precursor protein (APP) processing. J Exp Biol. 2009;212:494–8. doi: 10.1242/jeb.022780. [PubMed] [Cross Ref]
Li YM, Xu M, Lai MT, et al. Photoactivated gamma-secretase inhibitors directed to the active site covalently label presenilin 1. Nature. 2000;405:689–94. doi: 10.1038/35015085. [PubMed] [Cross Ref]
Lok K, Zhao H, Shen H, Lok K, Zhao H, Shen H, et al. Characterization of the APP/PS1 mouse model of Alzheimer's disease in senescence accelerated background. Neurosci Lett. 2013;557(Pt B):84–9. doi: 10.1016/j.neulet.2013.10.051. [PubMed] [Cross Ref]
Lok K, Zhao H, Zhang C, et al. Effects of accelerated senescence on learning and memory, locomotion and anxiety-like behavior in APP/PS1 mouse model of Alzheimer's disease. J Neurol Sci. 2013;335:145–54. doi: 10.1016/j.jns.2013.09.018. [PubMed] [Cross Ref]
Lucas JJ, Hernández F, Gómez-Ramos P, et al. Decreased nuclear beta-catenin, tau hyperphosphorylation and neurodegeneration in GSK-3beta conditional transgenic mice. EMBO J. 2001;20:27–39. doi: 10.1093/emboj/20.1.27. [PMC free article] [PubMed] [Cross Ref]
Manich G, Mercader C, del Valle J, et al. Characterization of amyloid-β granules in the hippocampus of SAMP8 mice. J Alzheimers Dis. 2011;25:535–46. [PubMed]
Markowska AL, Spangler EL, Ingram DK. Behavioral assessment of the senescence-accelerated mouse (SAM P8 and R1) Physiol Behav. 1998;64:15–26. doi: 10.1016/S0031-9384(98)00011-0. [PubMed] [Cross Ref]
McGowan E, Sanders S, Iwatsubo T, et al. Amyloid phenotype characterization of transgenic mice overexpressing both mutant amyloid precursor protein and mutant presenilin 1 transgenes. Neurobiol Dis. 1999;6:231–44. doi: 10.1006/nbdi.1999.0243. [PubMed] [Cross Ref]
Miyamoto M, Kiyota Y, Yamazaki N, et al. Age-related changes in learning and memory in the senescence-accelerated mouse (SAM) Physiol Behav. 1986;38:399–406. doi: 10.1016/0031-9384(86)90112-5. [PubMed] [Cross Ref]
Miyamoto M, Kiyota Y, Nishiyama M, Nagaoka A. Senescence-accelerated mouse (SAM): age-related reduced anxiety-like behavior in the SAM-P/8 strain. Physiol Behav. 1992;51:979–85. doi: 10.1016/0031-9384(92)90081-C. [PubMed] [Cross Ref]
Mondragón-Rodríguez S, Perry G, Luna-Muñoz J, et al. Phosphorylation of tau protein at sites Ser(396-404) is one of the earliest events in Alzheimer's disease and Down syndrome. Neuropathol Appl Neurobiol. 2013 [PubMed]
Morley JE, Kumar VB, Bernardo AE, et al. Beta-amyloid precursor polypeptide in SAMP8 mice affects learning and memory. Peptides. 2000;21:1761–7. doi: 10.1016/S0196-9781(00)00342-9. [PubMed] [Cross Ref]
Morley JE, Farr SA, Flood JF. Antibody to amyloid beta protein alleviates impaired acquisition, retention, and memory processing in SAMP8 mice. Neurobiol Learn Mem. 2002;78:125–38. doi: 10.1006/nlme.2001.4047. [PubMed] [Cross Ref]
Morley JE, Farr SA, Kumar VB, Armbrecht HJ. The SAMP8 mouse: a model to develop therapeutic interventions for Alzheimer's disease. Curr Pharm Des. 2012;18:1123–30. doi: 10.2174/138161212799315795. [PubMed] [Cross Ref]
Pallas M, Camins A, Smith MA, et al. From aging to Alzheimer's disease: unveiling "the switch" with the senescence-accelerated mouse model (SAMP8) J Alzheimers Dis. 2008;15:615–24. [PubMed]
Perry G, Raina AK, Nunomura A, et al. How important is oxidative damage? Lessons from Alzheimer's disease. Free Radic Biol Med. 2000;28:831–4. doi: 10.1016/S0891-5849(00)00158-1. [PubMed]

[Cross Ref]
Piedrahita D, Hernández I, López-Tobón A, et al. Silencing of CDK5 reduces neurofibrillary tangles in transgenic Alzheimer's mice. J Neurosci. 2010;30:13966–76. doi: 10.1523/JNEUROSCI.3637-10.2010. [PMC free article] [PubMed] [Cross Ref]
Pimplikar SW. Reassessing the amyloid cascade hypothesis of Alzheimer's disease. Int J Biochem Cell Biol. 2009;41:1261–8. doi: 10.1016/j.biocel.2008.12.015. [PMC free article] [PubMed] [Cross Ref]
Smith MA, Perry G, Richey PL, et al. Oxidative damage in Alzheimer's. Nature. 1996;382:120–1. doi: 10.1038/382120b0. [PubMed] [Cross Ref]
Swomley AM, Förster S, Keeney JT, et al. Abeta, oxidative stress in Alzheimer disease: evidence based on proteomics studies. Biochim Biophys Acta. 2013 [PMC free article] [PubMed]
Takeda T. Senescence-accelerated mouse (SAM) with special references to neurodegeneration models, SAMP8 and SAMP10 mice. Neurochem Res. 2009;34:639–59. doi: 10.1007/s11064-009-9922-y. [PubMed] [Cross Ref]
Takeda T, Hosokawa M, Takeshita S, et al. A new murine model of accelerated senescence. Mech Ageing Dev. 1981;17:183–94. doi: 10.1016/0047-6374(81)90084-1. [PubMed] [Cross Ref]
Thinakaran G, Borchelt DR, Lee MK, et al. Endoproteolysis of presenilin 1 and accumulation of processed derivatives in vivo. Neuron. 1996;17:181–190. doi: 10.1016/S0896-6273(00)80291-3. [PubMed] [Cross Ref]
Verri M, Pastoris O, Dossena M, et al. Mitochondrial alterations, oxidative stress and neuroinflammation in Alzheimer's disease. Int J Immunopathol Pharmacol. 2012;25:345–53. [PubMed]
Wisniewski HM, Wegiel J, Kotula L. Review: David Oppenheimer Memorial Lecture 1995: some neuropathological aspects of Alzheimer's disease and its relevance to other disciplines. Neuropathol Appl Neurobiol. 1996;22:3–11. doi: 10.1111/j.1365-2990.1996.tb00839.x. [PubMed] [Cross Ref]
Wolfe MS. Toward the structure of presenilin/γ-secretase and presenilin homologs. Biochim Biophys Acta. 2013;1828:2886–97. doi: 10.1016/j.bbamem.2013.04.015. [PMC free article] [PubMed] [Cross Ref]
Yagi H, Katoh S, Akiguchi I, Takeda T. Age-related deterioration of ability of acquisition in memory and learning in senescence accelerated mouse: SAM-P/8 as an animal model of disturbances in recent memory. Brain Res. 1988;474:86–93. doi: 10.1016/0006-8993(88)90671-3. [PubMed] [Cross Ref]
Zhu X, Raina AK, Perry G, Smith MA. Alzheimer's disease: the two-hit hypothesis. Lancet Neurol. 2004;3:219–26. doi: 10.1016/S1474-4422(04)00707-0. [PubMed] [Cross Ref]
Zhu X, Lee H, Perry G, Smith MA. Alzheimer disease, the two-hit hypothesis: an update. Biochim Biophys Acta. 2007;1772:494–502. doi: 10.1016/j.bbadis.2006.10.014. [PubMed] [Cross Ref]